*Appl. Math. Mech. -Engl. Ed.*, **40**(4), 579–590 (2019)

**Applied Mathematics and Mechanics (English Edition)**

https://doi.org/10.1007/s10483-019-2467-8

# Path integral solution of vibratory energy harvesting systems*

Wenan JIANG[1,†], Peng SUN[1], Gangling ZHAO[2], Liqun CHEN[3]

1. Department of Engineering Mechanics, Jiangsu University of Science and Technology, Zhenjiang 212003, Jiangsu Province, China;
2. School of Electronic and Electrical Engineering, Shangqiu Normal University, Shangqiu 476000, Henan Province, China;
3. Department of Mechanics, Shanghai University, Shanghai 200072, China

(Received May 2, 2018 / Revised Sept. 16, 2018)

**Abstract** A transition Fokker-Planck-Kolmogorov (FPK) equation describes the procedure of the probability density evolution whereby the dynamic response and reliability evaluation of mechanical systems could be carried out. The transition FPK equation of vibratory energy harvesting systems is a four-dimensional nonlinear partial differential equation. Therefore, it is often very challenging to obtain an exact probability density. This paper aims to investigate the stochastic response of vibration energy harvesters (VEHs) under the Gaussian white noise excitation. The numerical path integration method is applied to different types of nonlinear VEHs. The probability density function (PDF) from the transition FPK equation of energy harvesting systems is calculated using the path integration method. The path integration process is introduced by using the Gauss-Legendre integration scheme, and the short-time transition PDF is formulated with the short-time Gaussian approximation. The stationary probability densities of the transition FPK equation for vibratory energy harvesters are determined. The procedure is applied to three different types of nonlinear VEHs under Gaussian white excitations. The approximately numerical outcomes are qualitatively and quantitatively supported by the Monte Carlo simulation (MCS).

**Key words** nonlinear energy harvester, path integration, probability density function (PDF)

**Chinese Library Classification** O324, O316
**2010 Mathematics Subject Classification** 70K50

* Citation: JIANG, W. A., SUN, P., ZHAO, G. L., and CHEN, L. Q. Path integral solution of vibratory energy harvesting systems. *Applied Mathematics and Mechanics* (*English Edition*), **40**(4), 579–590 (2019) https://doi.org/10.1007/s10483-019-2467-8

† Corresponding author, E-mail: wenajiang@just.edu.cn

Project supported by the National Natural Science Foundation of China (Nos. 11702119 and 51779111) and the Natural Science Foundation of Jiangsu Province of China (Nos. BK20170565 and BK20170581)

## 1 Introduction

Vibration energy harvesters (VEHs) excited by random excitations have flourished as a focal research topic in recent years. Such sources of powers are currently finding applications in different fields of technology, such as wireless sensors, data transmitters, vivo biomedical implants, and health monitoring of structures and machines[1–5].

Many studies have been devoted to exploiting different random vibratory energy harvesting systems. Cottone et al.[6] found that the bistable oscillators can outperform the linear ones under the Gaussian white noise excitation. Daqaq[7] derived an approximate expression for the mean power under the exponentially correlated noise and demonstrated the existence of an optimal potential shape maximizing the output power. Green et al.[8] demonstrated that Duffing-type nonlinearities can reduce the size of electromagnetic energy harvesting devices. Daqaq[9] used the method of moment differential equations to calculate response statistics. Masana and Daqaq[10] investigated the influence of stiffness-type nonlinearities on the transduction of the buckling piezoelectric beam under the band-limited noise. He and Daqaq[11–12] employed the statistical linearization technique and the finite element method to investigate how the shape of the potential energy function influences the mean steady-state approximate output power. Xu et al.[13] introduced the stochastic averaging of energy envelope for Duffing-type VEHs. Kumar et al.[14] used the finite element method to solve the Fokker-Planck-Kolmogorov (FPK) equation of the associated bistable energy harvester. Jin et al.[15] introduced the equivalent nonlinearization technique to derive a semi-analytical solution of the corresponding nonlinear VEHs. Jiang and Chen[16–17] used the standard stochastic averaging method and the generalized stochastic averaging method to solve the response of nonlinear random vibratory energy harvesting systems. Liu et al. introduced VEHs with fractional-order nonlinear properties[18] and colored noise excitation[19], respectively. Xiao and Jin[20] proposed the energy harvester under the correlated white noise excitation, and computed the response with the generalized harmonic function method. Yang and Xu[21] exploited the VEHs with fractional derivative damping, and analyzed the dynamical response with the stochastic averaging method. As seen from the above description, the response statistical characteristics of random energy harvesting systems can be solved from the stationary FPK equation. However, to solve the probability density function (PDF) from the transition FPK equation has not been reported. To address the lack of studies in this aspect, the present work develops the path integration technique to solve the transient FPK equation.

The PDF evolution is governed by the FPK equation. Thus, the FPK equation provides a powerful tool for addressing the response characteristics of the nonlinear stochastic system. However, the FPK equation cannot be exactly solved. Many efforts have been devoted to developing different approximate or numerical approaches. Among various approaches[22–24], the path integration method has been receiving much attention, which can be traced back to Wehner and Wolfer[25], and also developed by Crandall et al.[26], Hsu and Chiu[27–28], Sun and Hsu[29], Naess and Johnson[30], Iourtchenkoa et al.[31] and Feng et al.[32]. Recently, a Gauss-Legendre integration scheme to improve the computational efficiency and accuracy of the path integration method was developed [33–34]. Subsequently, this approach was extended to the Duffing-Rayleigh oscillator[35], structural dynamic systems[36], and ship roll motion[37]. So far, to the authors' best knowledge, there is no path integration analysis on energy harvesting. To address the lack of studies in this aspect, the present work develops the path integration technique to determine the response of nonlinear energy harvesters under the Gaussian white noise excitation.

The paper is organized as follows. Section 2 reviews the governing equation of motion for vibratory energy harvesting systems. Section 3 establishes the PDF solution of vibratory energy harvesting systems under Gaussian noises excitations with the path integration method. Sections 4–6 investigate the stationary PDF solution of three different types of nonlinear VEHs.

Section 7 ends the paper with concluding remarks.

## 2 Vibration energy harvesting system

The electromechanical coupling equations of motion for vibration energy harvesting systems can be expressed as

$$m\ddot{\overline{x}} + c\dot{\overline{x}} + \frac{\mathrm{d}U(\overline{x})}{\mathrm{d}\overline{x}} + \chi\overline{z} = -m\ddot{\overline{x}}_{\mathrm{b}}, \tag{1}$$

$$C_{\mathrm{p}}\dot{\overline{z}} + \overline{z}/R = \chi\dot{\overline{x}} \text{ (piezoelectric)}, \quad L\dot{\overline{z}} + R\overline{z} = \chi\dot{\overline{x}} \text{ (electromagnetic)}, \tag{2}$$

where $x$ represents the displacement of the mass, $c$ is the damping coefficient, $\chi$ is the linear electromechanical coupling coefficient, $\ddot{x}_{\mathrm{b}}$ is the base acceleration, $C_{\mathrm{p}}$ is the capacitance, $L$ is the inductance, $U(\overline{x})$ represents the potential function symmetries and asymmetries, and $z$ is the electric quantity representing the induced voltage in piezoelectric harvesters and the induced current in the electromagnetic ones. These are measured across an equivalent resistive load $R$.

The non-dimensional electromechanical coupling equations can be described as[8–9]

$$\ddot{X} + 2\zeta\dot{X} + g(X) + \kappa Z = \xi(t), \tag{3}$$

$$\dot{Z} + \alpha Z = \dot{X}, \tag{4}$$

where $g(X) = \frac{\mathrm{d}U(\overline{x})}{\mathrm{d}\overline{x}}$, and $\xi(t) = -\ddot{x}_{\mathrm{b}}$ is the base acceleration. $\xi(t)$ is the Gaussian white noise with a zero mean and autocorrelation function

$$E[\xi(t)\xi(t+\tau)] = 2D\delta(\tau), \tag{5}$$

in which $E[\cdot]$ denotes the expected value, $D$ is the intensity of the excitation, and $\delta(\cdot)$ is the Dirac function.

It is worth noting that Eqs. (3)–(4) are universal since $g(X)$ represents the restoring force symmetries and asymmetries which include cubic nonlinearity, quadratic-cubic nonlinearity, and cubic-quintic nonlinearity.

The transition FPK equation corresponding to Eqs. (3) and (4) is governed as

$$\frac{\partial p(\boldsymbol{x},t)}{\partial t} = -\frac{\partial(f_1 p(\boldsymbol{x},t))}{\partial x} - \frac{\partial(f_2 p(\boldsymbol{x},t))}{\partial y} - \frac{\partial(f_3 p(\boldsymbol{x},t))}{\partial z} + D\frac{\partial^2 p(\boldsymbol{x},t)}{\partial x_2^2}, \tag{6}$$

where $\boldsymbol{x} = [x, y, z] = [X, \dot{X}, Z]$, $f_1 = y$, $f_2 = -(2\zeta y + g(x) + \kappa z)$, and $f_3 = -\alpha z + y$.

## 3 Path integration method for energy harvesting systems

For the PDF $p(x, y, z, t)$ at any given moment, it can be calculated through the integration from the transition probability density $q(x, y, z, t)$ and the initial distribution as

$$p(x,y,z,t) = \int_{\Omega} q(x,y,z,t|x^{(0)},y^{(0)},z^{(0)},t_0)p(x^{(0)},y^{(0)},z^{(0)},t_0)\mathrm{d}x^{(0)}\mathrm{d}y^{(0)}\mathrm{d}z^{(0)}, \tag{7}$$

where $\Omega$ is the integral interval of $x$, $y$, and $z$.

For a long-time duration into a sequence of appropriate short-time intervals from the initial distribution as follows:

$$\begin{aligned} p(x,y,z,t) = \int_{\Omega} \prod_{j=1}^{N} & q(x^{(j)},y^{(j)},z^{(j)},t_j|x^{(j-1)},y^{(j-1)},z^{(j-1)},t_{j-1}) \\ & \cdot p(x^{(j-1)},y^{(j-1)},z^{(j-1)},t_{j-1})\mathrm{d}x^{(j-1)}\mathrm{d}y^{(j-1)}\mathrm{d}z^{(j-1)}. \end{aligned} \tag{8}$$

Next, the Gauss-Legendre quadrature integration scheme is used to calculate Eq. (8). First, the domain along the $x$-direction is divided into two Gauss points as

$$\begin{cases} x_i = x_{\mathrm{L}} + 0.211\,3\,(x_{\mathrm{R}} - x_{\mathrm{L}}), \\ x_{i+1} = x_{\mathrm{R}} - 0.211\,3\,(x_{\mathrm{R}} - x_{\mathrm{L}}), \end{cases} \tag{9}$$

along the $y$-direction it can be discretized into

$$\begin{cases} y_i = y_{\mathrm{L}} + 0.211\,3\,(y_{\mathrm{R}} - y_{\mathrm{L}}), \\ y_{i+1} = y_{\mathrm{R}} - 0.211\,3\,(y_{\mathrm{R}} - y_{\mathrm{L}}), \end{cases} \tag{10}$$

and along the $z$-direction it can be written as

$$\begin{cases} z_i = z_{\mathrm{L}} + 0.211\,3\,(z_{\mathrm{R}} - z_{\mathrm{L}}), \\ z_{i+1} = z_{\mathrm{R}} - 0.211\,3\,(z_{\mathrm{R}} - z_{\mathrm{L}}). \end{cases} \tag{11}$$

In this case, the integral (8) can be discretized into the following composite Gauss-Legendre quadrature form:

$$\begin{aligned} p(x_r^I, y_s^I, z_t^I, t_I) =& \frac{\Delta_x}{2}\frac{\Delta_y}{2}\frac{\Delta_z}{2}\sum_{i=1}^{2n}\sum_{j=1}^{2m}\sum_{k=1}^{2l} q(x_i^I, y_j^I, z_k^I, t_I | x_i^{I-1}, y_j^{I-1}, z_k^{I-1}, t_{I-1}) \\ & \cdot p(x_i^{I-1}, y_j^{I-1}, z_k^{I-1}, t_{I-1}), \end{aligned} \tag{12}$$

where $\Delta_x$, $\Delta_y$, and $\Delta_z$ are the lengths of sub-intervals along the $x$-, $y$-, and $z$-directions, respectively.

The short time transition probability density is

$$q(x_i^I, y_j^I, z_j^I, t_I | x_i^{I-1}, y_j^{I-1}, z_j^{I-1}, t_{I-1}) = \frac{1}{(2\pi)^{3/2}|C|^{1/2}} \exp\Big(-\frac{1}{2}(\boldsymbol{x}^I - m_{\boldsymbol{x}^{I-1}})^{\mathrm{T}} C^{-1} (\boldsymbol{x}^I - m_{\boldsymbol{x}^{I-1}})\Big), \tag{13}$$

where $C = E[(\boldsymbol{x}^{I-1} - m_{\boldsymbol{x}^{I-1}})(\boldsymbol{x}^{I-1} - m_{\boldsymbol{x}^{I-1}})^{\mathrm{T}}]$, and $\boldsymbol{x}^{I-1} = [x_i^{I-1}, y_j^{I-1}, z_k^{I-1}]$.

Moreover, an initial distribution is selected as

$$p(x^{(0)}, y^{(0)}, z^{(0)}, 0) = \frac{1}{(2\pi)^{3/2}\sigma_x\sigma_y\sigma_z} \exp\Big(-\frac{(x^{(0)} - m_x)^2}{2\sigma_x^2} - \frac{(y^{(0)} - m_y)^2}{2\sigma_y^2} - \frac{(z^{(0)} - m_z)^2}{2\sigma_z^2}\Big), \tag{14}$$

where $m_x$, $m_y$, and $m_z$ are means, and $\sigma_x$, $\sigma_y$, and $\sigma_z$ are standard deviations.

## 4 Application to the Duffing-type VEH

The Duffing-type VEH is an important model of the nonlinear VEH, which had been widely reported[1]. Moreover, the non-dimensional electromechanical coupling equations can be described as

$$\ddot{X} + 2\zeta\dot{X} + X + \delta X^3 + \kappa Z = \xi(t), \tag{15}$$

$$\dot{Z} + \alpha Z = \dot{X}. \tag{16}$$

The transition probability in Eq. (13) is assumed to be Gaussian, and depends only on the mean and variances of $x$, $y$, and $z$. The mean and variances for the system can be derived from the non-dimensional electromechanical coupling equations (15) and (16), which yields

$$\begin{cases} \dot{m}_{100} = m_{010}, \\ \dot{m}_{010} = -2\zeta m_{010} - m_{100} - \delta m_{300} - \kappa m_{001}, \\ \dot{m}_{001} = m_{010} - \alpha m_{001}, \\ \dot{m}_{200} = 2m_{110}, \\ \dot{m}_{110} = m_{020} - 2\zeta m_{110} - m_{200} - \delta m_{400}, \\ \dot{m}_{101} = m_{011} + m_{110} - \alpha m_{101}, \\ \dot{m}_{020} = -4\zeta m_{020} - 2m_{110} - 2\delta m_{310} + 2D, \\ \dot{m}_{011} = -2\zeta m_{011} - m_{101} - \delta m_{301} + m_{020} - \alpha m_{011}, \\ \dot{m}_{002} = 2m_{011} - 2\alpha m_{002}, \end{cases} \tag{17}$$

where $m_{ijk} = E[x^i y^j z^k]$.

These moment equations are not closed because the system is nonlinear. The moments of higher than the second-order can be truncated by using the Gaussian closure procedure,

$$\begin{cases} m_{210} = m_{010}m_{200} + 2m_{100}m_{110} - 2m_{010}m_{100}^2, \\ m_{201} = m_{001}m_{200} + 2m_{100}m_{101} - 2m_{001}m_{100}^2, \\ m_{300} = 3m_{100}m_{200} - 2m_{100}^3, \\ m_{310} = 3m_{110}m_{200} - 2m_{010}m_{100}^3, \\ m_{301} = 3m_{101}m_{200} - 2m_{001}m_{100}^3, \\ m_{400} = 3m_{200}^2 - 2m_{100}^4, \\ m_{500} = 6m_{100}^5 - 20m_{100}^3 m_{200} + 15m_{100}m_{200}^2, \\ m_{510} = 16m_{010}m_{100}^5 - 10m_{110}m_{100}^4 - 20m_{010}m_{100}^3 m_{200} + 15m_{110}m_{200}^2, \\ m_{501} = 16m_{001}m_{100}^5 - 10m_{101}m_{100}^4 - 20m_{001}m_{100}^3 m_{200} + 15m_{101}m_{200}^2, \\ m_{600} = 16m_{100}^6 - 30m_{100}^4 m_{200} + 15m_{200}^3. \end{cases} \tag{18}$$

Substitute Eq. (18) into Eq. (17) and obtain the closed moment equations, i.e.,

$$\begin{cases} \dot{m}_{100} = m_{010}, \\ \dot{m}_{010} = -2\zeta m_{010} - m_{100} - \delta(3m_{100}m_{200} - 2m_{100}^3) - \kappa m_{001}, \\ \dot{m}_{001} = m_{010} - \alpha m_{001}, \\ \dot{m}_{200} = 2m_{110}, \\ \dot{m}_{110} = m_{020} - 2\zeta m_{110} - m_{200} - \delta(3m_{200}^2 - 2m_{100}^4), \\ \dot{m}_{101} = m_{011} + m_{110} - \alpha m_{101}, \\ \dot{m}_{020} = -4\zeta m_{020} - 2m_{110} - 2\delta(3m_{110}m_{200} - 2m_{010}m_{100}^3) + 2D, \\ \dot{m}_{011} = -2\zeta m_{011} - m_{101} - \delta(3m_{101}m_{200} - 2m_{001}m_{100}^3) + m_{020} - \alpha m_{011}, \\ \dot{m}_{002} = 2m_{011} - 2\alpha m_{002}. \end{cases} \tag{19}$$

Then, Eq. (19) can be solved by the fourth-order Runge-Kutta (RK4) algorithm. By substituting the solution of Eq. (19) into Eq. (13), the path integration PDFs can been calculated by using the initial distribution (14) and Eq. (12). The numerical implementation of the path integration method has been described above, and the main steps for the numerical implementation are concluded and given in Fig. 1.

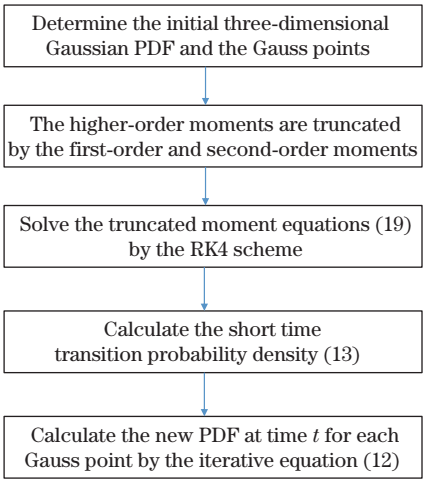


**Fig. 1** Flowchart of the numerical implementation of the three-dimensional path integration method

The PDFs and logarithmic PDFs of the displacement, velocity, and electricity obtained with the path integration method are compared with the Monte Carlo simulation (MCS) results of the systems (15) and (16) shown in Fig. 2. The system parameters are set as $\zeta = 0.8$, $\delta = 0.5$, $\kappa = 0.05$, $\alpha = 0.05$, and $D = 0.01$.

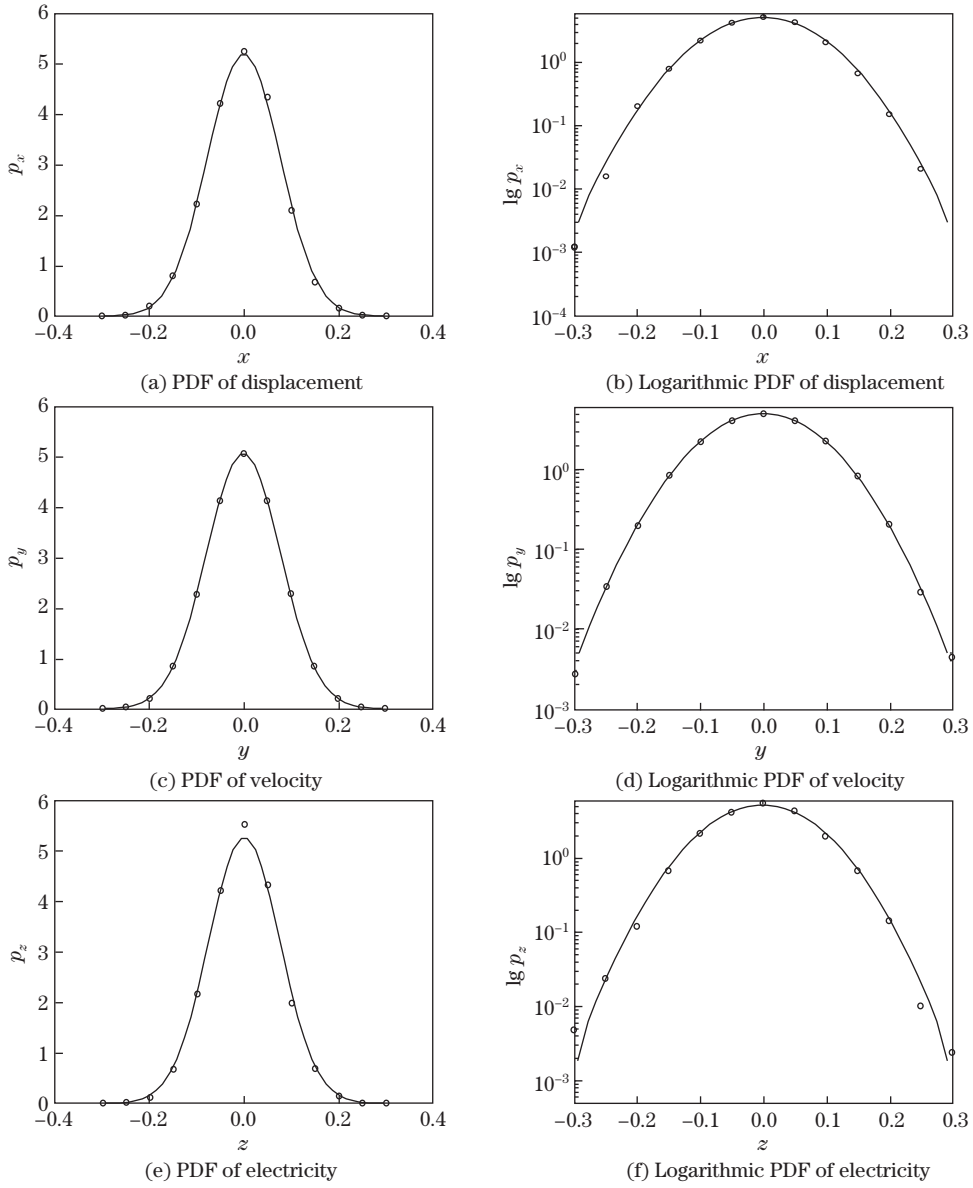


(a) PDF of displacement (b) Logarithmic PDF of displacement

(c) PDF of velocity (d) Logarithmic PDF of velocity

(e) PDF of electricity (f) Logarithmic PDF of electricity

**Fig. 2** Comparisons of PDFs and logarithmic PDFs of the Duffing-type VEH, in which the solid lines are numerical results from the path integration method, and the hollow circles are numerical results based on Eqs. (15) and (16) by using the RK4 algorithm

Figure 2 shows that the PDFs and logarithmic PDFs of displacement, velocity and electricity obtained with the path integration method are close to the MCS results. The logarithmic PDFs which show the effectiveness of the solution procedure can illustrate the accuracy of the tail region. The validity and accuracy of the path integration method have been verified by the MCS.

Figure 3 describes the joint PDFs of the displacement and velocity obtained with the path integration method and the MCS results of the systems (15) and (16). It is demonstrated that the joint PDF which is based on the path integration method agrees very well with the simulation result.

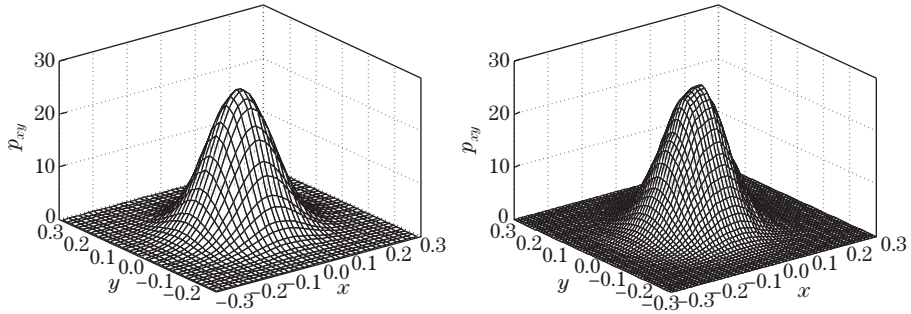


(a) Path integration method (b) MCS

**Fig. 3** Comparisons of stationary joint PDFs of the Duffing-type VEH

## 5 Application to the quadratic-cubic VEH

The quadratic-cubic VEH is an asymmetric system which includes quadratic and cubic nonlinearity in the restoring force[8]. One of the mathematical models for the quadratic-cubic VEH can be expressed as follows:

$$\ddot{X} + 2\zeta\dot{X} + X + \lambda X^2 + \delta X^3 + \kappa Z = \xi(t), \tag{20}$$

$$\dot{Z} + \alpha Z = \dot{X}. \tag{21}$$

The mean and variances for the system can be derived from the non-dimensional electromechanical coupling equations (20) and (21), which yields

$$\begin{cases} \dot{m}_{100} = m_{010}, \\ \dot{m}_{010} = -2\zeta m_{010} - m_{100} - \lambda m_{200} - \delta m_{300} - \kappa m_{001}, \\ \dot{m}_{001} = m_{010} - \alpha m_{001}, \\ \dot{m}_{200} = 2m_{110}, \\ \dot{m}_{110} = m_{020} - 2\zeta m_{110} - m_{200} - \lambda m_{300} - \delta m_{400}, \\ \dot{m}_{101} = m_{011} + m_{110} - \alpha m_{101}, \\ \dot{m}_{020} = -4\zeta m_{020} - 2m_{110} - 2\lambda m_{210} - 2\delta m_{310} + 2D, \\ \dot{m}_{011} = -2\zeta m_{011} - m_{101} - \lambda m_{201} - \delta m_{301} + m_{020} - \alpha m_{011}, \\ \dot{m}_{002} = 2m_{011} - 2\alpha m_{002}, \end{cases} \tag{22}$$

where $m_{ijk} = E[x^i y^j z^k]$.

Substitute Eq. (18) into Eq. (22) and obtain closed moment equations by the RK4 algorithm. The system parameters are selected as $\zeta = 0.2$, $\delta = 0.5$, $\kappa = 0.5$, $\alpha = 0.5$, $\lambda = 1$, and $D = 0.01$. Therefore, the path integration PDFs can be rendered by using the initial distribution (14) and Eq. (12).

Figure 4 depicts the PDFs and logarithmic PDFs of the displacement, velocity, and electricity for the quadratic-cubic VEH, and Fig. 5 shows the joint PDFs of displacement and velocity obtained with the path integration method and the MCS results of the systems (20) and (21). These results show that the approximate PDFs and logarithmic PDFs of the path integration method coincide with the MCS ones.

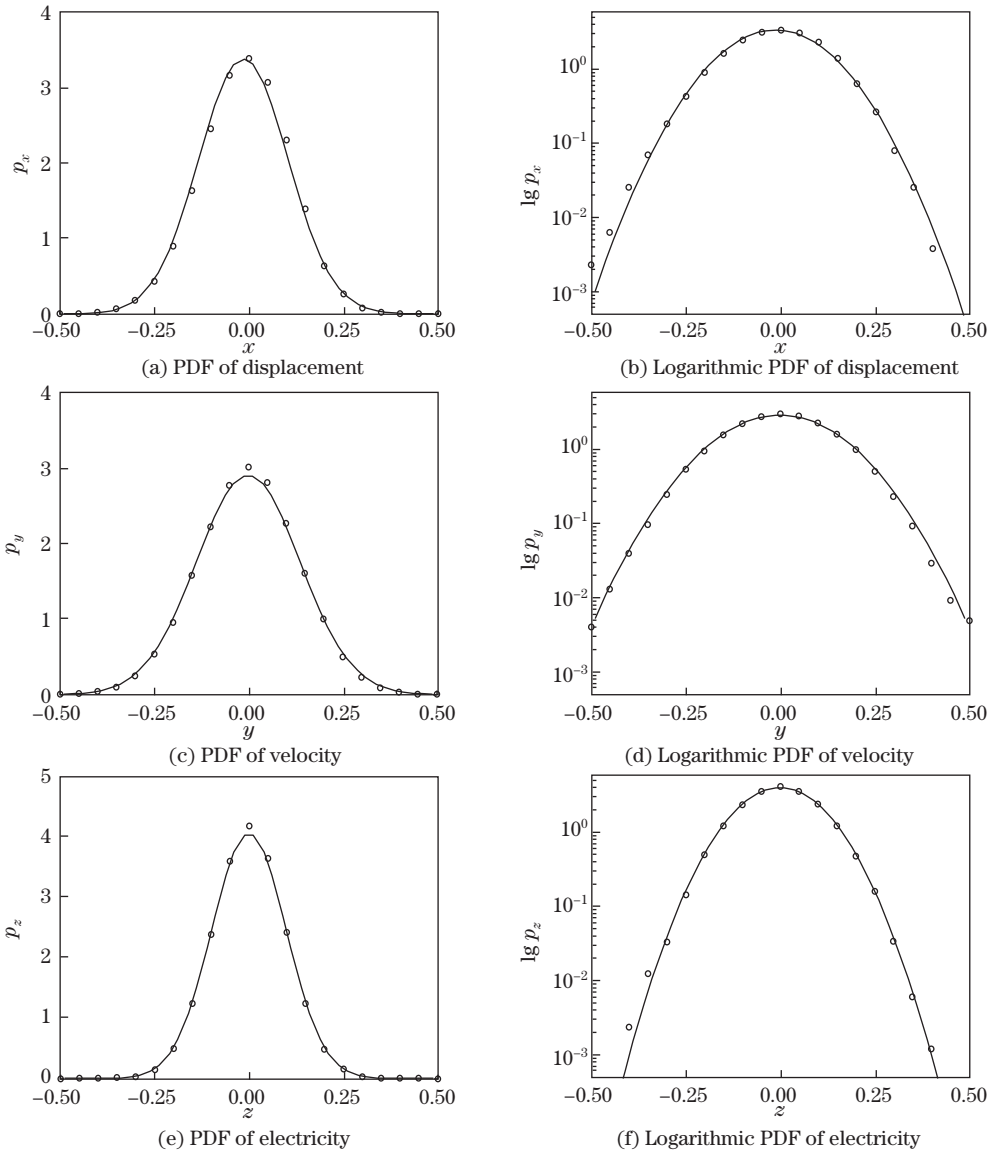


**Fig. 4** Comparisons of PDFs and logarithmic PDFs of the quadratic-cubic VEH, in which the solid lines are numerical results from the path integration method, and the hollow circles are numerical results based on Eqs. (20) and (21) by using the RK4 algorithm

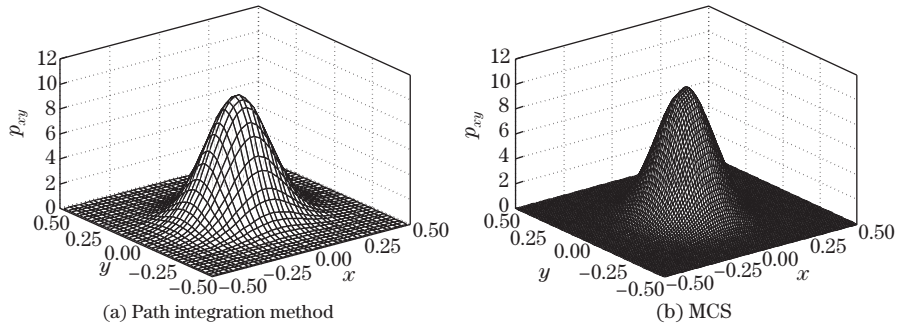


**Fig. 5** Comparisons of stationary joint PDFs of the quadratic-cubic VEH

## 6 Application to cubic-quintic VEH

A cubic-quintic Duffing-type VEH was designed by Cao et al.[38], and they discussed the influence of the potential well depth on the harvesting performance under the harmonic excitation. Jiang and Chen[17] investigated the stochastic response of the cubic-quintic Duffing-type VEH under the Gaussian white noise excitation by using the stochastic averaging method. The non-dimensional electromechanical coupling equations can be written as

$$\ddot{X} + 2\zeta\dot{X} + X + \delta X^3 + \beta X^5 + \kappa Z = \xi(t), \tag{23}$$

$$\dot{Z} + \alpha Z = \dot{X}. \tag{24}$$

The transition probability in Eq. (13) is assumed to be Gaussian, and depends only on the mean and variances of $x$, $y$, and $z$. The mean and variances for the system can be derived from the non-dimensional electromechanical coupling equations (23) and (24), which yields

$$\begin{cases} \dot{m}_{100} = m_{010}, \\ \dot{m}_{010} = -2\zeta m_{010} - m_{100} - \delta m_{300} - \beta m_{500} - \kappa m_{001}, \\ \dot{m}_{001} = m_{010} - \alpha m_{001}, \\ \dot{m}_{200} = 2m_{110}, \\ \dot{m}_{110} = m_{020} - 2\zeta m_{110} - m_{200} - \delta m_{400} - \beta m_{600}, \\ \dot{m}_{101} = m_{011} + m_{110} - \alpha m_{101}, \\ \dot{m}_{020} = -4\zeta m_{020} - 2m_{110} - 2\delta m_{310} - 2\beta m_{510} + 2D, \\ \dot{m}_{011} = -2\zeta m_{011} - m_{101} - \delta m_{301} - \beta m_{501} + m_{020} - \alpha m_{011}, \\ \dot{m}_{002} = 2m_{011} - 2\alpha m_{002}, \end{cases} \tag{25}$$

where $m_{ijk} = E[x^i y^j z^k]$.

These moment equations are not closed because the system is nonlinear. The moments of higher than the second-order can be truncated by using the Gaussian closure procedure. By substituting Eq. (18) into Eq. (25) and obtaining closed moment equations, the path integration PDFs can be calculated with the closed moment. The system parameters are selected as $\zeta = 0.4$, $\delta = 5$, $\kappa = 0.05$, $\alpha = 0.05$, $\beta = 1$, and $D = 0.01$.

For the cubic-quintic VEH, the PDFs and logarithmic PDFs of the displacement, velocity, and electricity obtained with the path integration method are compared with the MCS results in Fig. 6, and the joint PDFs of displacement and velocity are presented in Fig. 7. The PDFs and logarithmic PDFs obtained from the path integration agree well with the MCS ones.

## 7 Conclusions

In this paper, we investigate the response of the vibration-based energy harvester under the Gaussian white noise. To achieve this goal, the path integration solution of the transition FPK equation of energy harvesting systems is used to obtain the response statistics of the harvester. The path integration process is determined by using the Gauss-Legendre integration scheme, and the short-time transition PDF is introduced by the short-time Gaussian approximation. The procedure is applied to three different types of nonlinear VEHs under Gaussian white excitations. It is observed that, both of the path integration solution and the direct Monte Carlo numerical integration of the stochastic differential equations provide close predictions for the marginal PDFs of the displacement, velocity, and electricity, and the joint PDFs of the displacement and velocity.

The investigation yields the following conclusions.

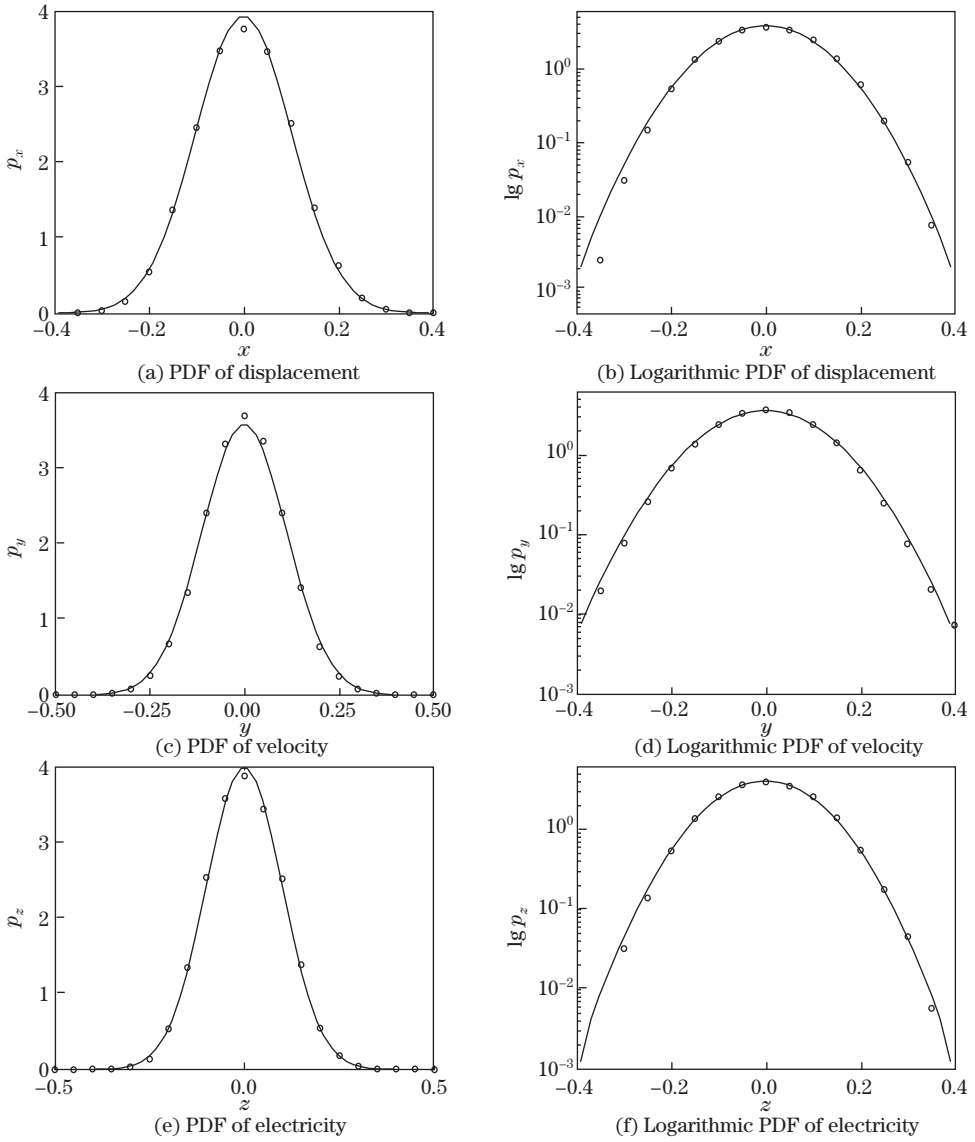


**Fig. 6** Comparisons of PDFs and logarithmic PDFs of the cubic-quintic VEH, in which the solid lines are numerical results from the path integration method, and the hollow circles are numerical results based on Eqs. (23) and (24) by using the RK4 algorithm

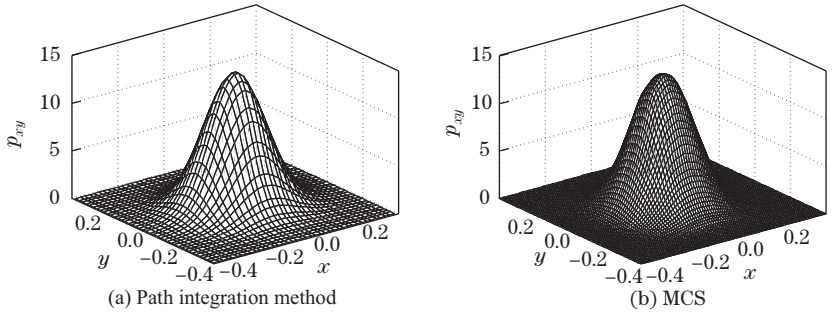


**Fig. 7** Comparisons of stationary joint PDFs of the cubic-quintic VEH

(I) The information of how probability distribution evolves over time is formulated numerically by the values of transition PDF at the discrete Gaussian quadrature points.

(II) The PDF from the transition FPK equation of energy harvesting systems is obtained.

(III) The path integration outcomes are qualitatively and quantitatively supported by the MCS.

## References


[1] DAQAQ, M. F., MASANA, R., ERTURK, A., and QUINN, D. D. On the role of nonlinearities in vibratory energy harvesting: a critical review and discussion. *Applied Mechanics Reviews*, **66**, 040801 (2014)

[2] ELVIN, N. and ERTURK, A. *Advances in Energy Harvesting Methods*, Springer, New York (2013)

[3] WANG, H. R., XIE, J. M., XIE, X., HU, Y. T., and WANG, J. Nonlinear characteristics of circular-cylinder piezoelectric power harvester near resonance based on flow-induced flexural vibration mode. *Applied Mathematics and Mechanics* (*English Edition*), **35**, 229–236 (2014) https://doi.org/10.1007/s10483-014-1786-6

[4] HAJHOSSEINI, M. and RAFEEYAN, M. Modeling and analysis of piezoelectric beam with periodically variable cross-sections for vibration energy harvesting. *Applied Mathematics and Mechanics* (*English Edition*), **37**, 1053–1066 (2016) https://doi.org/10.1007/s10483-016-2117-8

[5] LI, X., ZHANG, Y. W., DING, H., and CHEN, L. Q. Integration of a nonlinear energy sink and a piezoelectric energy harvester. *Applied Mathematics and Mechanics* (*English Edition*), **38**, 1019–1030 (2017) https://doi.org/10.1007/s10483-017-2220-6

[6] COTTONE, F., VOCCA, H., and GAMMAITONI, L. Nonlinear energy harvesting. *Physical Review Letters*, **102**, 080601 (2009)

[7] DAQAQ, M. F. Transduction of a bistable inductive generator driven by white and exponentially correlated Gaussian noise. *Journal of Sound and Vibration*, **330**, 2554–2564 (2011)

[8] GREEN, P. L., WORDEN, K., ATALLAH, K., and SIMS, N. D. The benefits of Duffing-type nonlinearities and electrical optimisation of a mono-stable energy harvester under white Gaussian excitations. *Journal of Sound and Vibration*, **331**, 4504–4517 (2012)

[9] DAQAQ, M. F. On intentional introduction of stiffness nonlinearities for energy harvesting under white Gaussian excitations. *Nonlinear Dynamics*, **69**, 1063–1079 (2012)

[10] MASANA, R. and DAQAQ, M. F. Response of Duffing-type harvesters to band-limited noise. *Journal of Sound and Vibration*, **332**, 6755–6767 (2013)

[11] HE, Q. F. and DAQAQ, M. F. Influence of potential function asymmetries on the performance of nonlinear energy harvesters under white noise. *Journal of Sound and Vibration*, **33**, 3479–3489 (2014)

[12] HE, Q. F. and DAQAQ, M. F. New insights into utilizing bistability for energy harvesting under white noise. *Journal of Vibration and Acoustics*, **137**, 021009 (2015)

[13] XU, M., JIN, X. L., WANG, Y., and HUANG, Z. L. Stochastic averaging for nonlinear vibration energy harvesting system. *Nonlinear Dynamics*, **78**, 1451–1459 (2014)

[14] KUMAR, P., NARAYANAN, S., ADHIKARI, S., and FRISWELL, M. I. Fokker-Planck equation analysis of randomly excited nonlinear energy harvester. *Journal of Sound and Vibration*, **333**, 2040–2053 (2014)

[15] JIN, X. L., WANG, Y., XU, M., and HUANG, Z. L. Semi-analytical solution of random response for nonlinear vibration energy harvesters. *Journal of Sound and Vibration*, **340**, 267–282 (2015)

[16] JIANG, W. A. and CHEN, L. Q. Stochastic averaging of energy harvesting systems. *International Journal of Non-Linear Mechanics*, **85**, 174–187 (2016)

[17] JIANG, W. A. and CHEN, L. Q. Stochastic averaging based on generalized harmonic functions for energy harvesting systems. *Journal of Sound and Vibration*, **377**, 264–283 (2016)

[18] LIU, D., XU, Y., and LI, J. L. Randomly-disordered-periodic-induced chaos in a piezoelectric vibration energy harvester system with fractional-order physical properties. *Journal of Sound and Vibration*, **399**, 182–196 (2017)

[19] LIU, D., XU, Y., and LI, J. L. Probabilistic response analysis of nonlinear vibration energy harvesting system driven by Gaussian colored noise. *Chaos, Solitons & Fractals*, **104**, 806–812 (2017)

[20] XIAO, S. M. and JIN, Y. F. Response analysis of the piezoelectric energy harvester under correlated white noise. *Nonlinear Dynamics*, **90**, 2069–2082 (2017)

[21] YANG, Y. G. and XU, W. Stochastic analysis of monostable vibration energy harvesters with fractional derivative damping under Gaussian white noise excitation. *Nonlinear Dynamics*, **94**(1), 639–648 (2018)

[22] SUN, Y., HONG, L., JIANG, J., and LI, Z. Estimation of critical conditions for noise-induced bifurcation in nonautonomous nonlinear systems by stochastic sensitivity function. *International Journal of Bifurcation and Chaos*, **26**, 1650184 (2016)

[23] CHEN, L. C., LIU, J., and SUN, J. Q. Stationary response probability distribution of SDOF nonlinear stochastic systems. *Journal of Applied Mechanics*, **84**, 051006 (2017)

[24] SUN, Y., HONG, L., YANG, Y., and SUN, J. Q. Probabilistic response of nonsmooth nonlinear systems under Gaussian white noise excitations. *Physica A*, **508**, 111–117 (2018)

[25] WEHNER, M. F. and WOLFER, W. G. Numerical evaluation of path-integral solution to Fokker-Plank equations. *Physical Review A*, **27**, 2663–2670 (1983)

[26] CRANDALL, S. H., CHANDIRAMANI, K. L., and COOK, R. G. Some first-passage problems in random vibration. *Journal of Applied Mechanics*, **33**, 532–538 (1966)

[27] HSU, C. S. and CHIU, H. M. A cell mapping method for non-linear deterministic and stochastic systems I: the method of analysis. *Journal of Applied Mechanics*, **53**, 695–701 (1986)

[28] HSU, C. S. and CHIU, H. M. A cell mapping method for nonlinear deterministic and stochastic systems II: examples of application. *Journal of Applied Mechanics*, **53**, 702–710 (1986)

[29] SUN, J. Q. and HSU, C. S. The generalized cell mapping method in nonlinear random vibration based upon short-time Gaussian approximation. *Journal of Applied Mechanics*, **57**, 1018–1025 (1990)

[30] NAESS, A. and JOHNSON, J. M. Response statistics of nonlinear, compliant offshore structures by the path integral solution method. *Probabilistic Engineering Mechanics*, **8**, 91–106 (1993)

[31] IOURTCHENKOA, D. V., MO, E., and NAESS, A. Response probability density functions of strongly non-linear systems by the path integration method. *International Journal of Non-Linear Mechanics*, **41**, 693–705 (2006)

[32] FENG, G. M., WANG, B., and LU, Y. F. Path integral, functional method, and stochastic dynamical systems. *Probabilistic Engineering Mechanics*, **7**, 149–157 (1992)

[33] YU, J. S., CAI, G. Q., and LIN, Y. K. A new path integration procedure based on Gauss-Legendre scheme. *International Journal of Non-Linear Mechanics*, **32**, 759–768 (1997)

[34] YU, J. S. and LIN, Y. K. Numerical path integration of a non-homogeneous Markov process. *International Journal of Non-Linear Mechanics*, **39**, 1493–1500 (2004)

[35] XIE, W. X., XU, W., and CAI, L. Study of the Duffing-Rayleigh oscillator subject to harmonic and stochastic excitations by path integration. *Applied Mathematics and Computation*, **172**, 1212–1224 (2006)

[36] WANG, Y. A path integration algorithm for stochastic structural dynamic systems. *Applied Mathematics and Computation*, **228**, 423–431 (2014)

[37] ZHU, H. T. and DUAN, L. L. Probabilistic solution of non-linear random ship roll motion by path integration. *International Journal of Non-Linear Mechanics*, **83**, 1–8 (2016)

[38] CAO, J. Y., ZHOU, S. X., WANG, W., and LIN, J. Influence of potential well depth on nonlinear tristable energy harvesting. *Applied Physics Letters*, **106**, 173903 (2015)